UNCLASSIFIED

Defense Technical Information Center Compilation Part Notice

ADP010901

TITLE: Self-Organized Criticality Models of Neural Development

DISTRIBUTION: Approved for public release, distribution unlimited

This paper is part of the following report:

TITLE: Paradigms of Complexity. Fractals and Structures in the Sciences

To order the complete compilation report, use: ADA392358

The component part is provided here to allow users access to individually authored sections of proceedings, annals, symposia, ect. However, the component should be considered within the context of the overall compilation report and not as a stand-alone technical report.

The following component part numbers comprise the compilation report:

ADP010895 thru ADP010929

UNCLASSIFIED

SELF-ORGANIZED CRITICALITY MODELS OF NEURAL DEVELOPMENT

D.L. RAIL

Neurology Department, Campbelltown Hospital, Campbelltown NSW 2560, Australia
Email: drail@talent.com.au

B.I. HENRY AND S.D.WATT

Department of Applied Mathematics, School of Mathematics,
University of New South Wales, Sydney NSW 2052, Australia
E-mail: B.Henry@unsw.edu.au, S.Watt@unsw.edu.au

A simple evolutionary model is introduced for neural development along the lines of the Bak-Sneppen model for biological evolution of an ecology. The model represents a set of neurons and their connections together with associated synaptic weights. Evolution of the system is studied for different model fitness functions of the synaptic weights. The model systems exhibit Darwinian evolution of the synaptic weight space towards maturation.

1 Introduction

Until recently the biological contribution to learning was thought to be an unfolding according to an intrinsic schedule [1,2]. However, evidence now indicates that the developing cerebral cortex is largely free of domain-specific structure [3,4] and the representational properties of the cortex are built by the nature of the problems confronting it.

At the neurobiological level, learning stems from the interaction between intrinsic growth and environmentally derived activity [4]. Two factors that are fundamental for this interaction are selection and variance. Selection [5,6,7,8] has two distinct stages. The first stage constructs "pre-representations". The second stage selectively eliminates certain of these representations. The most fit representations survive to underlie mature skills.

Variation is important for the development of a maximally flexible representation capacity. The florid growth of neural tissues in ontogeny [4]: synapses; axonal and dendritic arborisation represents one possibility for introducing a significant chance element to learning. Representations are consolidated by a gradual increase in the synaptic weights of preferred units (synaptic weight space). The widely accepted mechanism for such consolidation is Hebbian learning via positive reinforcement. At the neural net level, Hebbian learning follows from the covariance of pre- and post-synaptic discharges. At the circuit level, it involves synergy of oscillators involved in common function. Synapses which do not participate in the maintenance of circuits are eliminated.

Selectivity and variability are also important aspects of biological evolution. One of the simplest models for biological evolution is the Bak-Sneppen model [9]. In this model evolutionary activity is simulated through random mutations of the least fit species and its neighbours. A characteristic feature of this model is that it exhibits Self-Organized Criticality whereby the system evolves through a succession

of punctuated equilibria to a state where almost all species have fitness above a threshold level.

In this paper we have introduced new variants of the Bak-Sneppen model to investigate the evolution of synaptic weight space towards maturation in simple models for neural development.

2 Neural Connectivity Model

Consider a set of n units (neurons) labelled $1, 2, 3, \ldots, n$ on a periodic one-dimensional lattice, i.e., units $k+1$ and $k-1$ are neighbours of unit k which is equivalent to unit $n+k$. Associated with each unit k we identify a set of $c(k)$ connections (synapses). Two versions of the models are studied. One in which the number of connections is kept fixed ($c(k) = m$) and the other in which the number of connections (for the least fit unit and its two neighbours) is selected at random, ($c(k) \in [1, m]$) at each update step. We have in mind that the former situation will be easier to investigate theoretically whereas the latter will be more representative of a model neural system. Let $c_j(k)$ denote the jth connection associated with unit k and identify a corresponding synaptic weight $a \leq w_j(k) \leq b$. Pre-representations are introduced by choosing the synaptic weight for each connection at random from a uniform distribution in the range $[a, b]$. Initially we suppose that the system is fully connected, i.e., initially $c(k) = m$ for all k. There is no discernible difference in the long term results whether or not the system is initially randomly connected. Selection and variation in the system is modelled by replacing the least fit unit and its two neighbours by new units with new randomly assigned connections and weights.

Three different models have been examined. In Model A the weights are random numbers in the range $[0, 1]$ and the fitness of a unit is defined as the minimum weight for that unit. In Model B the weights are random numbers in the range $[-1, 1]$ and the fitness of a unit is defined as the average of the weights for that unit. In Model C the weights are again random numbers in the range $[-1, 1]$ but the fitness is defined as the sum of the weights. The choice of the range $[-1, 1]$ in the latter two models is to include the possibility of both excitatory and inhibitory synapses. In each model the steps in the update procedure are as follows:

1. Set up the pre-representations which are fully connected with random synaptic weights.

2. Calculate the fitness for each unit and identify the unit with the lowest fitness.

3. For the least fit unit and each of its neighbouring units reset the number of connections depending on the variant of the model and assign new weights at random from a uniform distribution on $[a, b]$.

4. Return to step 2 and continue for N updates.

Model A with $m = 1$ is the Bak-Sneppen model. The transient behaviour of this model is characterized by punctuated equilibria as the system evolves towards a statistically stationary state in which the density of weights in the system with

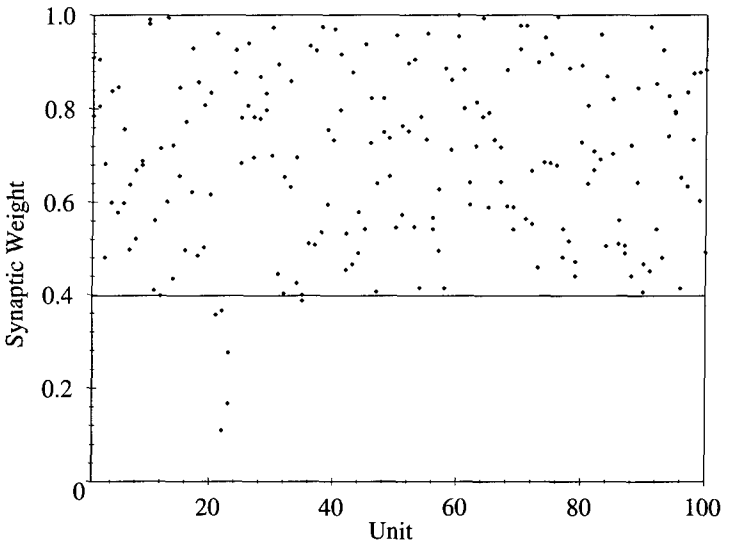

Figure 1. Snapshot of the stationary state for Model A with $m = 2$ and fixed numbers of connections.

$w < w^*$ vanishes. The critical weight $w^* \sim 0.66702 \pm 0.00003$ [10] is referred to as the self-organized threshold. A plot of the largest value of the minimum weight after s updates versus s reveals a staircase structure where the average length of a step in the staircase scales as a power law distribution. The change in the minimum weight across a level step in the staircase is referred to as an avalanche [9].

3 Simulations

Simulations of the models have been carried out for $n = 100$ units and $s = 10^6$ updates over a range of values of the maximum number of connections $m \in [1, 2^{10}]$; both for fixed number of connections and for random numbers of connections (up to the maximum m). To facilitate the discussion of these results let $f_m(s)$ denote the fitness of the least fit unit after the sth update in a model where m is the maximum number of connections.

In all cases the transient behaviour exhibits punctuated equilibria and the long term behaviour is highly correlated with almost all fitness values above a critical value. Figure 1 shows the weights for each unit plotted against the unit number in the 'stationary state', after 10^4 updates, in Model A with $m = 2$ and the number of connections fixed. Except for the localized avalanche, all weights are above the limiting threshold weight. Similar long term trends are found in all cases independent of m (compare for example, Figure 1 of [11] which shows a similar plot for the original Bak-Sneppen model), however the magnitude of the limiting threshold fitness is m dependent.

The transient behaviours with their characteristic punctuated equilibria are shown for each of the models in Figures 2a,2b,3a,3b,3c. These figures show plots of

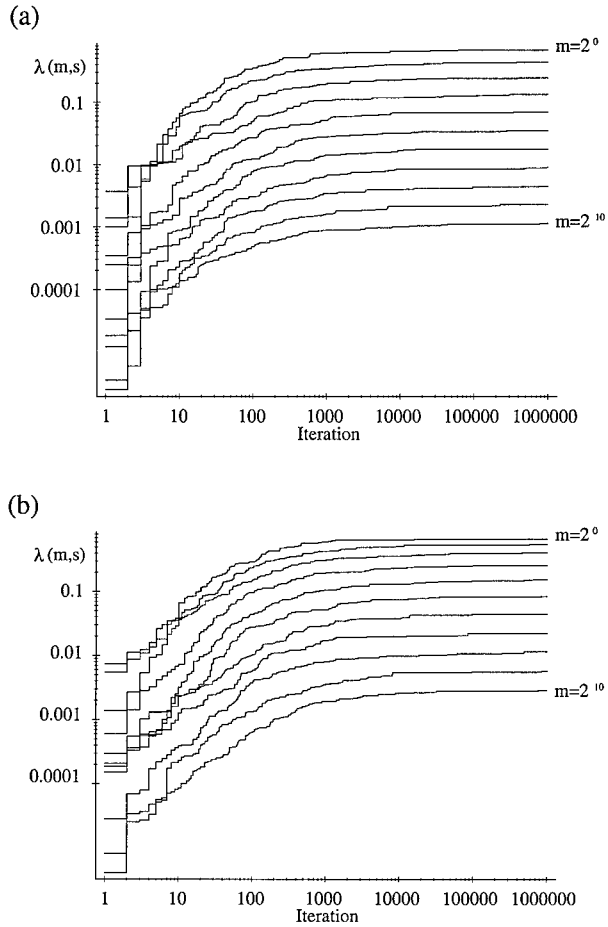

Figure 2. Devil's staircase structure for Model A; (a) fixed numbers of connections, (b) random numbers of connections.

the maximum value of the minimum fitness after s updates,

$$\lambda(m, s) = \max_{[0,s]} f_m(s),$$

versus s. In each horizontal step of the staircase structure in these figures the minimum fitness remains less than this threshold value. A rise in the staircase occurs when the minimum fitness exceeds this threshold value. The case of Model B with fixed numbers of connections was not simulated because this is the same as Model C with fixed numbers of connections apart from the scale factor m (see further comments below).

In Models A and B the limiting threshold fitness,

$$\lambda^*(m) = \lim_{s\to\infty} \max_{[0,s]} f_m(s),$$

decreases with an increase in the maximum number of connections m. In Model C

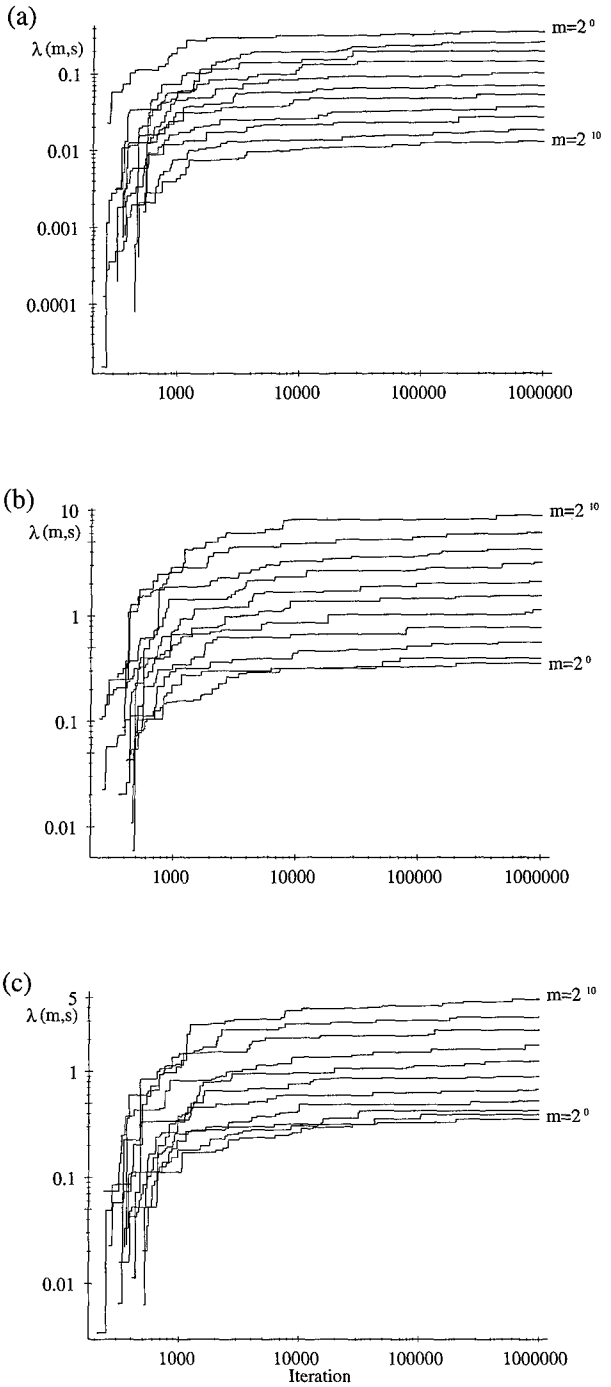

Figure 3. Devil's staircase structure; (a) Model B with random numbers of connections; (b) Model C with fixed numbers of connections, (c) Model C with random numbers of connections.

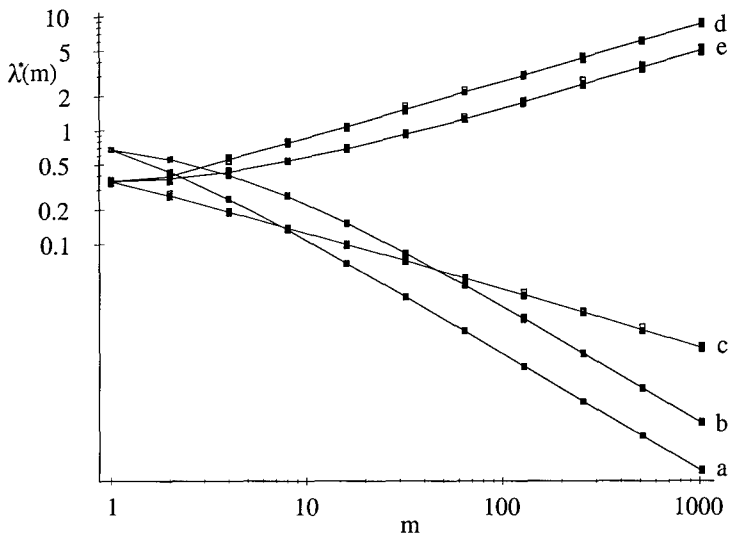

Figure 4. Plot of the limiting threshold fitness versus the maximum number of connections m: (a) Model A with fixed numbers of connections; (b) Model A with random numbers of connections; (c) Model B with random numbers of connections; (d) Model C with fixed numbers of connections; (e) Model C with random numbers of connections.

the opposite is true. Figure 4 shows plots of the limiting threshold fitness $\lambda^*(m)$ versus m for each of the models. The error bars in the plots are based on data from ten runs of each model and the lines are ensemble averages. From these plots we note that for large m: $\lambda^*(m) \sim \frac{1}{m}$ - for Model A; $\lambda^*(m) \sim \frac{1}{\sqrt{m}}$ - for Model B; and $\lambda^*(m) \sim \sqrt{m}$ - for Model C. For Model A the limiting value $\lambda^*(1)$ is the Bak-Sneppen self-organized criticality threshold value 0.66702.... For models B and C the limiting value $\lambda^*(1) \approx 2 \times 0.66702 - 1 = 0.33404$.

4 Scaling Analysis

The functional relationships between the limiting threshold fitness (the self-organized threshold) and the maximum numbers of connections can be obtained using simple probabilistic arguments. To this end (following [12]) we first define the avalanche probability function, $P_{\lambda(m)}(s)$ as the probability for an avalanche with threshold fitness $\lambda(m)$ which starts at $k = 0$ to end at $k = s$. It follows immediately from the definition that $P_{\lambda(m)}(0) = 0$. In Model A, the probability for the avalanche to end at step $k + 1$ is

$$P_{\lambda_A(m)}(k+1) = (1 - P_{\lambda_A(m)}(k))(1 - \lambda_A(m))^{3m}. \tag{1}$$

The first factor on the right hand side is the probability that the avalanche did not stop at the earlier step k and the factor $(1 - \lambda_A(m))^{3m}$ is the probability of independently selecting new fitness values at random from a uniform distribution for each of the $3m$ connections, for the least fit unit and its two neighbours, above

the threshold fitness $\lambda_A(m)$. It is a straightforward exercise to obtain the solution to the difference equation, Eq.(1). The solution for initial condition $P_{\lambda_A(m)}(0) = 0$ is

$$P_{\lambda_A(m)}(k) = \frac{(1-\lambda_A(m))^{3m}}{1+(1-\lambda_A(m))^{3m}}(1-(-1)^k(1-\lambda_A(m))^{3mk}). \tag{2}$$

At the limiting threshold values $\lambda_A^*(m)$ we anticipate that the avalanche probabilities $P_{\lambda_A^*(m)}(k)$ are independent of m. In particular by equating $P_{\lambda_A^*(m)}(k) = P_{\lambda_A^*(1)}(k)$ we obtain the relation

$$\lambda_A^*(m) = 1-(1-\lambda_A^*(1))^{\frac{1}{m}}, \tag{3}$$

where $\lambda_A^*(1)$ is the limiting threshold fitness for the Bak-Sneppen model. The agreement between Eq. (3) and the values plotted in Figure 4 is summarized in Table 1.

We now consider the scaling relation for model C. In this case the avalanche probabilities are determined by the equation

$$P_{\lambda_C(m)}(k+1) = (1-P_{\lambda_C(m)}(k))(1-\Phi\left(\frac{\lambda_C(m)}{\sqrt{m}\sigma}\right))^3 \tag{4}$$

where

$$\Phi(x) = \frac{1}{\sqrt{2\pi}}\int_{-\infty}^{x}\exp\left(-\frac{z^2}{2}\right)dz.$$

The second factor on the right hand side of Eq.(4) follows from the Central Limit Theorem. For sufficiently large m, the sum $Y(m)$ of m random numbers from a uniform distribution with zero mean and variance σ^2 is a Gaussian random variable Z with zero mean and variance $m\sigma^2$. Hence the probability of randomly selecting the sum $Y(m) \geq \lambda_C(m)$ is equal to the probability of selecting the Gaussian random variable $Z \geq \frac{\lambda_C(m)}{\sqrt{m}\sigma}$. This probability is given by

$$1-\Phi\left(\frac{\lambda_C(m)}{\sqrt{m}\sigma}\right).$$

The solution of Eq.(4) for initial condition $P_{\lambda_C(m)}(0) = 0$ is

$$P_{\lambda_C(m)}(k) = \frac{(1-\Phi\left(\frac{\lambda_C(m)}{\sqrt{m}\sigma}\right))^3}{1+(1-\Phi\left(\frac{\lambda_C(m)}{\sqrt{m}\sigma}\right))^3}(1-(-1)^k(1-\Phi\left(\frac{\lambda_C(m)}{\sqrt{m}\sigma}\right))^{3k}). \tag{5}$$

The avalanche probabilities given by Eq.(5) are approximations based on the Central Limit Theorem which holds with increasing accuracy as m increases. The approximation is already reasonable for $m \geq 2$ but it does not hold in the case $m = 1$ where the sum over m random numbers from a uniform distribution on $[-1, 1]$ is simply the uniform random variable. In this case the probability for choosing a random variable greater than $\lambda_C(1)$ is $(1-\lambda_C(1))/2$ so that the avalanche probability is given by

$$P_{\lambda_C(1)}(k) = \frac{(\frac{1-\lambda_C(1)}{2})^3}{1+(\frac{1-\lambda_C(1)}{2})^3}(1-(-1)^k(\frac{1-\lambda_C(1)}{2})^{3k}). \tag{6}$$

Table 1. Comparison between limiting threshold fitness values; $\tilde{\lambda}(m)$ obtained from the numerical simulations, and $\lambda(m)$ obtained from the theoretical scaling relations Eqs.(3,7). The percentage difference between these values is also shown.

m	$\lambda_A^*(m)$	$\tilde{\lambda}_A^*(m)$	% diff.	$\lambda_C^*(m)$	$\tilde{\lambda}_C^*(m)$	% diff.
1	0.67789	0.67789	0.00	0.35751	—	—
2	0.43259	0.43245	0.03	0.39351	0.39351	0.00
4	0.24769	0.24664	0.42	0.55863	0.55650	0.38
8	0.13330	0.13203	0.95	0.77354	0.78701	1.74
16	0.06815	0.06835	0.29	1.07521	1.11300	3.51
32	0.03501	0.03478	0.65	1.52210	1.57402	3.41
64	0.01774	0.01754	1.13	2.17175	2.22601	2.50
128	0.00884	0.00881	0.36	3.01230	3.14805	4.51
256	0.00442	0.00441	0.29	4.29448	4.45201	3.67
512	0.00222	0.00221	0.53	6.09033	6.29610	3.38
1024	0.00111	0.00110	0.47	8.49563	8.90402	4.81

The limiting threshold value for $m = 1$ in Model C is given by $\lambda_C^*(1) = 2\lambda_A^*(1) - 1$. To obtain the scaling behaviour with m of the limiting threshold values $\lambda_C^*(m)$ for $m \geq 2$ we now equate $P_{\lambda_C^*(m)}(k) = P_{\lambda_C^*(2)}(k)$ which yields

$$\lambda_C^*(m) = \sqrt{\frac{m}{2}}\lambda_C^*(2). \tag{7}$$

The good agreement between the $\lambda_C^*(m)$ values plotted in Figure 4 for $m \geq 2$ and Eq.(7) is summarized in Table 1.

The scaling behaviour in the case of model B can be obtained by repeating the analysis for model C but replacing $\Phi\left(\frac{\lambda_C(m)}{\sqrt{m}\sigma}\right)$ by $\Phi\left(\frac{\sqrt{m}\lambda_B(m)}{\sigma}\right)$ since the average of m random numbers from a uniform distribution with zero mean and variance σ^2 is a Gaussian random variable with zero mean and variance σ^2. This yields the scaling result

$$\lambda_B^*(m) = \sqrt{\frac{2}{m}}\lambda_B^*(2). \tag{8}$$

5 Discussion

The simple evolutionary models for neural development introduced in this paper attempt to model the chance aspect of learning via Darwinian evolution. All models exhibit Darwinian evolution of the synaptic weight space towards maturation where almost all neurons have fitness levels above a threshold value.

It is anticipated that the maximum number of connections scales with memory and learning. With this interpretation the 'fitness' functions in each of the models needs some clarification since from Figure 4 and the scaling analysis above we see that only Model C exhibits an increase of fitness with increasing memory and

learning. On this basis the fitness function in Model C is more representative of learning and memory than the fitness function in Models A and B. However a fitness function that scales with memory and learning can also be recovered from the present fitness function in models A and B simply by multiplying by an appropriate monotonically increasing function of m. For example multiply by m^γ where; $\gamma > 1$ for Model A, $\gamma > 1/2$ for Model B, and $\gamma > 0$ for Model C.

It is interesting that the scaling relations: $\lambda_A^*(m) \sim 1/m$, $\lambda_B^*(m) \sim 1/\sqrt{m}$ and $\lambda_C^*(m) \sim \sqrt{m}$ which were derived in the theoretical analysis (and obtained numerically) for the case of fixed numbers of connections are also obtained in our numerical simulations when the numbers of connections is selected at random (for the least fit unit and its neighbours) in each update. With the appropriate interpretation of fitness as above, for a fixed maximum number of connections, we find that the neurons self-organize themselves to operate at increasing fitness whilst at the same time decreasing the numbers of active connections. The scaling analysis of this reduction in the number of active connections with increasing fitness is deserving of further studies.

Towards the end of this study we became aware of the neuronal model of self-organized learning recently introduced by Chialvo and Bak [13]. Our models are similar to their model to the extent that memory and learning is consolidated via Darwinian elimination of the least fit units rather than via Hebbian re-inforcement of the most fit units. On the other hand our models are more crude than the Chialvo-Bak model since we do not include the dynamics of firing in our models.

References

1. E.H. Lenneberg, *Biological Foundations of Language* (Wiley, 1967).
2. N. Chomsky, *Behavioral and Brain Sciences* **3** 1 (1980).
3. W.T. Greenough, J.E. Black and C.S. Wallace, *Child Development* **58**, 539 (1987).
4. S. R. Quartz and T. J. Sejnowski, *Behavioral and Brain Sciences* **20**, 537 (1997).
5. N. Jerne in *The Neurosciences: A Study Program*, ed. G.C. Quarton, T. Melnechuk, F.O. Schmitt (Rockefeller University Press, 1967).
6. J.P. Changeux and A. Danchin, *Nature* **264**, 705 (1976).
7. P. Rakic, J. P. Bourgeois, M.F. Eckenhoff, N. Zecevic and P. S. Goldman-Rakic. *Science* **232**, 232 (1986).
8. G. M. Edelman, *Neural Darwinism. The Theory of Neuronal Group Selection* (Basic Books, 1987).
9. P. Bak and K. Sneppen, *Phys. Rev. Letts.* **71**, 4083 (1993).
10. M. Paczuski, S. Maslov, and P. Bak, *Phys. Rev. E* **53**, 414 (1996).
11. P. Bak and S. Boettcher, *Physica D* **107**, 143 (1997).
12. S. Boettcher and M. Paczuski, *Phys. Rev. Letts* **76**, 348 (1996).
13. D. Chialvo and P. Bak, *Neuroscience* **90**, 1137 (1999).